https://doi.org/10.5194/acp-2019-866
Preprint. Discussion started: 16 October 2019

Atmospheric Chemistry and Physics Discussions

Missing OH Reactivity in the Global Marine Boundary Layer

Alexander B. Thames[1], William H. Brune[1], David O. Miller[1], Hannah M. Allen[4], Eric C. Apel[2], Donald R. Blake[15], T. Paul Bui[8], Roisin Commane[14], John D. Crounse[4], Bruce C. Daube[13], Glenn S. Diskin[5], Joshua P. DiGangi[5], James. W. Elkins[10], Samuel. R. Hall[2], Thomas F. Hanisco[6], Reem A. Hannun[6;7], Eric Hintsa[10;12], Rebecca S. Hornbrook[2], Michelle J. Kim[3], Kathryn McKain[10;12], Fred L. Moore[10;12], Julie M. Nicely[6;7], Jeffrey Peischl[10;11], Thomas B. Ryerson[11], Jason M. St. Clair[6;7], Colm Sweeney[9], Alex Teng[4], Chelsea R. Thompson[16;11;12], Kirk Ullmann[2], Paul O. Wennberg[3], and Glenn M. Wolfe[6;7]

[1]Department of Meteorology and Atmospheric Science, The Pennsylvania State University, University Park, PA, USA.
[2]Atmospheric Chemistry Observations and Modeling Laboratory, National Center for Atmospheric Research, Boulder, CO, USA.
[3]Division of Geological and Planetary Sciences, California Institute of Technology, Pasadena, CA, USA.
[4]Division of Chemistry and Chemical Engineering, California Institute of Technology, Pasadena, CA, USA.
[5]Chemistry and Dynamics Branch, NASA Langley Research Center, Hampton, VA, USA.
[6]Atmospheric Chemistry and Dynamics Laboratory, NASA Goddard Space Flight Center, Greenbelt, MD, USA.
[7]Joint Center for Earth Systems Technology, University of Maryland, Baltimore County, Catonsville, MD, USA.
[8]Earth System Science Interdisciplinary Center, University of Maryland, College Park, MD, USA
[9]Earth Science Division, NASA Ames Research Center, Moffett Field, CA, USA.
[10]Global Monitoring Division, NOAA Earth System Research Laboratory, Boulder, CO, USA.
[11]Chemical Sciences Division, NOAA Earth System Research Laboratory, Boulder, CO, USA.
[12]Cooperative Institute for Research in Environmental Sciences, University of Colorado, Boulder, CO, USA.
[13]Department of Earth and Planetary Sciences, Harvard University, Cambridge, MA, USA.
[14]Department of Earth and Environmental Sciences, Lamont-Doherty Earth Observatory, Columbia University, Palisades, NY, USA.
[15]Department of Chemistry, University of California, Irvine, CA, USA.
[16]Now with Scientific Aviation, Boulder, CO, USA.

Correspondence to: William H. Brune (whb2@psu.edu)

Abstract. The hydroxyl radical (OH) reacts with thousands of chemical species in the atmosphere, initiating their removal and the chemical reaction sequences that produce ozone, secondary aerosols, and gas-phase acids. OH reactivity, which is the inverse of OH lifetime, influences the OH abundance and the ability of OH to cleanse the atmosphere. The NASA Atmospheric Tomography (ATom) campaign used instruments on the NASA DC-8 aircraft to measure OH reactivity and more than 100 trace chemical species. ATom presented a unique opportunity to test the completeness of the OH reactivity calculated from the chemical species measurements by comparing it to the measured OH reactivity over two oceans across four seasons. Although the calculated OH reactivity was below the OH reactivity instrument's limit-of-detection for much of the free troposphere, the OHR instrument was able to measure the OH reactivity in and just above the marine boundary layer. The average measured value of OH reactivity in the marine boundary layer across all latitudes and all ATom phases was 1.9 s^{-1}, which 0.5 s^{-1} larger than the average calculated OH reactivity. Concurrently, missing OH reactivity, the difference between the measured and calculated OH reactivity, was measured to be ~0.5-2.0 s^{-1} at some locations in the

https://doi.org/10.5194/acp-2019-866
Preprint. Discussion started: 16 October 2019

Atmospheric Chemistry and Physics Discussions

tropics and midlatitudes. Correlations of missing OH reactivity with formaldehyde, dimethyl sulfide, butanal, and sea surface temperature suggest the presence of unmeasured or unknown volatile organic compounds or oxygenated volatile organic compounds associated with ocean emissions.

1 Introduction

The primary fate of the thousands of trace gases emitted into the atmosphere is chemical reaction with hydroxyl (OH). While OH is produced primarily by the photolysis of ozone, followed by a reaction between excited-state atomic oxygen and water vapor, OH is lost by the sum of the reaction frequencies with these trace gases. This sum of losses is called the OH reactivity and has units of s^{-1}. If OH production remains constant, increases in OH reactivity will decrease the total atmospheric OH concentration. Thus, understanding global OH reactivity is a key to understanding global OH and the global atmospheric oxidation capacity.

An important example is methane (CH_4), which is removed from the atmosphere primarily by reaction with OH. Two estimates of the CH_4 lifetime due to oxidation by OH are 9.7 ± 1.5 years (Naik et al., 2013) and 11.2 ± 1.3 years (Prather et al., 2012). A recent global inverse analysis of GOSAT satellite CH_4 column emissions finds a CH_4 lifetime of 10.8 ± 0.4 years for oxidation by tropospheric OH (Maasakkers et al., 2019), which is within the uncertainties of the other two estimates. Understanding the CH_4 lifetime depends on understanding global spatial and temporal OH distribution, which is strongly influenced by the spatial and temporal distribution of OH reactivity.

OH reactivity is the inverse of the OH lifetime. It is calculated as a sum of the reaction frequencies of OH reactants multiplied by their reaction rate coefficients:

$$k_{OH} = \sum_i k_{(OH+X_i)}[X_i]. \quad (1)$$

where $k_{(OH+X_i)}$ represents some species X's reaction rate coefficient with OH and $[X_i]$ is the concentration of that species. If there is no OH production, then the equation for the OH decay is

$$\frac{d[OH]}{dt} = -k_{OH}[OH]. \quad (2)$$

The first direct measurements of OH reactivity were made in Nashville, TN in summer 1999 (Kovacs et al., 2003). The measured OH reactivity exceeded the calculated by about 30%, which was thought to come from short-lived highly reactive VOCs that were not measured in that study. The difference between the measured and calculated OH reactivity was referred to as the "missing" OH reactivity. For forest environments, the first evidence for missing OH reactivity came from direct OH reactivity measurements in northern Michigan forest in summer 2000 (Di Carlo et al., 2004). As much as a third of the OH

https://doi.org/10.5194/acp-2019-866
Preprint. Discussion started: 16 October 2019

Atmospheric Chemistry and Physics Discussions

reactivity was missing, with missing OH reactivity increasing with temperature in a manner identical to the expected increase of forest monoterpene emissions. Since then, OH reactivity has been measured many times in various urban, rural, and forest environments (Yang et al., 2016, and references therein). The fraction of missing OH reactivity in different forests varies from less than 20%, which is approximately the uncertainty in the measured and calculated OH reactivity (Kaiser et al., 2016; Zannoni et al., 2016), to more than 50% (Nölscher et al., 2012; Nölscher et al., 2016). Considering the large numbers of trace gases emitted into the atmosphere (Goldstein and Galbally, 2007), it is possible that missing OH reactivity comes from OH reactants that were not measured or not included in previously calculated totals of the OH reactivity sum. In some studies, the OH reactants have been only those that were measured, and in other studies unmeasured but modeled OH reactants – such as organic peroxyl radicals and oxygenated volatile organic compound (OVOC) products – have been included. A recent intercomparison of several OH reactivity instruments demonstrated that these large missing OH reactivity values are probably not due to instrument issues (Fuchs et al., 2017). These discrepancies have yet to be resolved.

One regime that has yet to be adequately investigated is the remote marine boundary layer (MBL) and the free troposphere above it, which comprises 70% of the global lower troposphere. Two prior studies measured OH reactivity in the MBL. The most recent was shipborne across the Mediterranean Sea, through the Suez Canal, and into the Arabian Gulf in summer 2017 (Pfannerstill et al., 2019). Median measured OH reactivity for the different waterways ranged from 6 s^{-1} to 13 s^{-1}, while median calculated OH reactivity ranged from 2 s^{-1} to 9 s^{-1}. Missing OH reactivity was more than 4 s^{-1} in air masses affected by pollution, although the calculated OH reactivity of ~2 s^{-1} was below the instrument's limit of detection (LOD) in the cleaner portions of the Mediterranean and Adriatic Seas.

The other study involved airborne OH reactivity measurements made during the Intercontinental Chemical Transport Experiment Phase B (INTEX-B) study, a NASA airborne campaign investigating Asian-influenced pollution over the north Pacific Ocean in April-May, 2006 (Mao et al., 2009). At altitudes below ~2 km, missing OH reactivity was ~2.4 s^{-1}, more than the calculated OH reactivity of 1.6 ± 0.4 s^{-1}. It decreased to within measurement uncertainty above 4 km. The correlation of missing OH reactivity with formaldehyde (HCHO) suggested that the missing OH reactivity was due to highly reactive VOCs that had HCHO as a reaction product. The confinement of the missing OH reactivity to the MBL and just above it suggested that cause of the missing OH reactivity was ocean emissions of volatile organic compounds (VOCs).

In this paper, we describe measurements of OH reactivity that were made during the NASA Atmospheric Tomography (ATom) campaign (ATom, 2016). This campaign took place in four month-long phases, each in a different season, between August 2016 and May 2018 and covered nearly all latitudes over the Pacific and Atlantic Oceans. Although the calculated OH reactivity in the middle-to-upper troposphere is less than the OH reactivity instrument's LOD of ~0.4 s^{-1} at 1σ confidence, this instrument can measure OH reactivity in and just above the MBL. The comprehensive instrument suite

https://doi.org/10.5194/acp-2019-866
Preprint. Discussion started: 16 October 2019

Atmospheric Chemistry and Physics Discussions

105 deployed aboard the NASA DC-8 airborne laboratory allows a detailed examination of which trace gases most influence measured OH reactivity.

2 Methods

Here we discuss the ATom campaign, the OH reactivity instrument and its measurement capabilities, the model used to
110 generate calculated OH reactivity, and the statistical analysis that was used to find correlations with missing OH reactivity.

2.1 ATom

The ATom campaign consisted of four deployments over all four seasons, starting with northern hemisphere summer in 2016 and ending with northern hemisphere spring in 2018 (Table 1).

115 Each deployment used the NASA DC-8 Airborne Science Laboratory (DC-8) to profile the atmosphere by frequently ascending and descending between 0.2 km and 12 km on flights north from California to Alaska, down the Pacific to New Zealand, across the Antarctic Circle to Chile, up the Atlantic Ocean to Greenland, across the Arctic Circle to Alaska and then back to California (yellow lines in Fig. 1). As shown in Table 2, the DC-8 carried a suite of instruments that measured over 100 different chemical constituents, aerosol particle properties and chemical composition, photolysis frequencies, and
120 meteorological variables (ATom, 2016).

2.2 OH Reactivity Measurement

The OH reactivity concept and the basic instrument has been described before for ground-based operation (Kovacs and Brune, 2001) and for aircraft operation (Mao et al., 2009). The instrument used for ATom, called OHR, is a version of the one described by Mao et al. (2009). A brief description of the concept and the instrument is presented below.

125

Sampled air is brought into the instrument during flight by ram force at the 1.2 cm diameter inlet and the Venturi effect at the instrument outlet. A movable wand at the center of a flow tube (7.5 cm dia.) injects OH into the flow tube at different distances from an OH detection inlet and axis similar to the one used to detect OH in the atmosphere. In the wand, OH is generated in a flow of humidified carrier (N_2 or purified air), which is exposed to 185 nm radiation from a Hg lamp that
130 photolyzes the H_2O to make OH and HO_2. As the wand moves away from the detection axis, the signal observed of unreacted OH with the sample air decreases. Assuming a constant decay rate, measured OH reactivity is determined by Eq. (3):

$$k_{OH} = \frac{ln\left(\frac{[OH_o]}{[OH]}\right)}{\Delta t} - k_{background} \quad (3)$$

https://doi.org/10.5194/acp-2019-866
Preprint. Discussion started: 16 October 2019

Atmospheric Chemistry and Physics Discussions

where [OH] is the instantaneous OH concentration, $[OH_0]$ is the initial OH concentration, Δt is reaction time between the [OH] measurements (the distance the wand moves divided by the flow speed), and $k_{background}$ is the instrument background due to OH loss to the walls or to impurities in the carrier gas. The wand moves approximately 10 cm in total along its path from closest point to farthest point from the detection axis. The sampling time step is synced with the Airborne Tropospheric Hydrogen Oxides Sensor (ATHOS, an instrument used in tandem with the OHR instrument to measure in situ OH and HO_2), which samples at 5 Hz. Depending on the ATom phase, the wand takes 15 or 20 seconds to move 10 cm and back to its starting position, where it rests for 5 or 10 seconds while the OH detection system measures the background signal. Flow speeds through the OHR instrument are measured with a hot-wire anemometer and are typically between 0.25 m s^{-1} at lower altitudes and 0.45 m s^{-1} at higher altitudes, resulting in a typical total measured reaction time between 0.40 and 0.20 seconds.

It is important to note that all OH reactivity instruments measure the "instantaneous" OH reactivity, which is only the reactions that occur within the maximum reaction time observed by that instrument. This maximum time is typically less than a second. These instruments do not measure either subsequent OH reactivity or OH production if the time constants for that chemistry are greater than the maximum reaction time. In relatively clean environments, no subsequent chemistry affects the measured OH decay. However, in high NO environments, the reaction $HO_2 + NO \rightarrow OH + NO_2$ is fast enough to convert HO_2 to OH, thereby altering the observed OH decay. No high NO environments were encountered in ATom.

In all previous ground-based and aircraft-based studies, high purity N_2 was used as the carrier gas in the wand. During aircraft-based studies, a cylinder of N_2 gas was consumed on each 8-hour flight and accordingly had to be replaced before the next flight. It was not possible to position caches of N_2 cylinders at each of the ~12 layovers during each ATom phase. Instead of N_2, air from a zero-air generator (PermaPure ZA-750-12) was used as the carrier gas in the laboratory prior to ATom. Before each mission, the zero-air generator media was replaced and the air produced by the unit was verified to be pure by running it through a Potential Aerosol Mass chamber that rapidly oxidizes any VOCs to particles (Lambe et al., 2011). No particles were seen, indicating that the air had negligible amounts of larger reactive VOCs. The exception to this procedure was during ATom4, when the zero-air generator itself had to be replaced late in instrument integration period. The media was changed prior to the ATom4 integration and the research flights, but the air purity was unable to be checked until after the ATom4 phase had ended, when it was found that the OHR background was higher than in previous ATom phases.

The OHR background varied throughout the campaign due to subtle changes in the zero-air generator performance and between research flights due to internal contamination from pre-flight conditions. These variations were tracked with measurements of the OHR instrument background in the laboratory and, for ATom4, in situ during several flights. For the laboratory calibrations, the internal pressure of the OHR instrument was varied between 25 and 100 kPa to simulate in-flight conditions. For the in situ calibrations taken during the second half of ATom4, the OHR instrument was switched from

https://doi.org/10.5194/acp-2019-866
Preprint. Discussion started: 16 October 2019

Atmospheric Chemistry and Physics Discussions

sampling the ambient flow to sampling high purity N_2 from a reserve N_2 cylinder. The flow rate out of the cylinder was adjusted to match the flow speed measured by the hot-wire anemometer just prior to the switch. During ascent and descent, the internal pressure and flow speed changed too quickly over the length of one decay to get a good background calibration, so background calibrations were taken only from stable altitude legs, predominantly at the low altitudes.

Two complete laboratory calibrations, the in situ calibration, and two calibrations only at ~100 kPa were used to determine $k_{background}$ for the different ATom phases (Fig. 2). The 2017 calibration applies to ATom2 and ATom3, while the 2018 calibration applies to ATom1 and ATom4. At ~1000 hPa pressure, the standard deviation is $\pm$0.3 s^{-1} for the laboratory calibrations and $\pm$0.8 s^{-1} for the in situ calibrations. The difficulty of maintaining steady calibration conditions in flight causes the larger in situ calibration error. The excellent agreement between the laboratory and in situ background calibrations for ATom4 confirms the finding of Mao et al. (2009) that laboratory background calibrations before or after a campaign accurately capture the instrument background during the campaign. All calibrations are pressure-dependent, with all three background calibrations being the same to within 0.5 s^{-1} at 300 hPa instrument flow tube pressure, which is approximately 10 km altitude. This observed pressure dependence of the background calibration is different from the behavior of the pressure-independent background calibration used by Mao et al. (2009). However, a re-examination of the Mao et al. (2009) data indicates that the background during INTEX-B was also pressure dependent, with a background of 2.9 s^{-1} at low altitudes and 2.0 s^{-1} at high altitudes, nearly identical to the values used for ATom2 and ATom3.

The OHR background varied slightly from flight to flight because the variable air quality produced by the zero-air generator. This flight-to-flight variation was tracked and the OH reactivity background was corrected by the following procedure. The OH reactivity calculated from the model at the OHR instrument's temperature and pressure (sec Sect 2.3) was 0.25-0.30 s^{-1} for the upper troposphere during all ATom phases and latitudes. Even if there was 0.3 s^{-1} of missing OH reactivity in the upper troposphere, this amount is below the LOD for the OHR instrument, which is ~0.4 s^{-1} for 1-minute sums. Therefore, the background calibrations were adjusted in the range of ±0.34 s^{-1} for each research flight by a pressure-invariant offset that was necessary to make the measured and model calculated OH reactivity the same near the tropopause. In effect, we used the upper troposphere as a clean standard in order to fine-tune $k_{background}$, just as Mao et al. (2009) did.

The OH signals in the upper troposphere were high enough to allow the slopes of the OH decays to be determined with good precision for each 20-30 s decay. However, at the low altitudes, quenching of the fluorescence signal by higher air and water vapor abundances reduced the OH signals. To compensate for this reduction, decays were binned into 1-minute sums before the decay slopes were calculated. Three OH signal decays from low altitudes during ATom2 are shown in Fig. 3. When $k_{background}$ is subtracted from the decays shown in Fig. 3, their values become ~5 s^{-1} (blue), ~3 s^{-1} (teal), and ~2 (yellow) s^{-1}.

https://doi.org/10.5194/acp-2019-866
Preprint. Discussion started: 16 October 2019

Atmospheric Chemistry and Physics Discussions

At all pressures, the background calibration data indicate that the backgrounds are known to ±0.4 s^{-1} at 1σ confidence. The uncertainty in decay fit is approximately 7.5% at the 1σ confidence level, such that the total uncertainty can be found by Eq. (4).

$$\Delta k_{OH} = \sqrt{(0.4)^2 + (k_{OH} * 0.075)^2} \quad (4)$$

For example, for a measured decay of 5 s^{-1}, the resulting uncertainty would be ±0.55 s^{-1} at 1σ confidence. Therefore, in each ATom phase, the total uncertainty in the OH reactivity is dominated by the instrument background uncertainty.

The calculated OH reactivity rarely exceeded 2 s^{-1} in the planetary boundary and was only 0.2 s^{-1} in the free troposphere. These low values presented a significant challenge for our OHR instrument, as it would have for any OH reactivity instrument; even the most precise instrument measuring in a chamber at its home laboratory has a LOD of ±0.2 s^{-1}, 1σ confidence, for a measurement integration time of 60-160 seconds (Fuchs et al., 2017). If the same instrument were to sample air masses on an aircraft traveling 200 m s^{-1}, its precision would likely be degraded. From this perspective, the LOD on these ATom measurements is about as low as that for any other OH reactivity measurements.

The analysis in the paper is focused on the first three ATom phases. ATom4 is excluded from this analysis for two reasons. First, background calibrations were performed during more than half of the low-altitude periods over the Atlantic, severely limiting the ambient measurements in the MBL. Second, the increased contamination during ATom4 made the OH reactivity measurements 2-3 times noisier than during the previous ATom phases.

2.3 Photochemical Box Model

The photochemical box model used to calculate OH reactivity is the Framework for 0-D Atmospheric Modeling (F0AM) (Wolfe et al, 2016). It uses the Master Chemical Mechanism v3.3.1 (MCMv331) for all gas-phase reactions (Jenkin et al., 1997; Saunders et al., 2003). Both the F0AM model framework and MCMv3.3.1 are publicly available. The reactions of CH_3O_2 + OH and $C_2H_5O_2$ + OH were added to the model mechanism with rate coefficients from Assaf et al. (2017). The model was run with the integration time set to 3 days with a first-order dilution lifetime of 12 hours, although the calculated OH reactivity was the same to within a few percent for an order-of-magnitude change in these times. The model was constrained by the simultaneous measurements listed in Table 2. These measurements were taken from the 1-second merge file, averaged to 1-minute values, and interpolated to a common 1-minute time step. In cases where multiple measurements of a chemical species exist (e.g., CO), a primary measurement was chosen and other measurements were used to fill gaps in the primary measurement.

https://doi.org/10.5194/acp-2019-866
Preprint. Discussion started: 16 October 2019

Atmospheric Chemistry and Physics Discussions

The OHR flow tube temperature and pressure were used to calculate reaction rate coefficients and reactant concentrations to compare with the observations. Equation 1 was then used to find the model calculated OH reactivity. If the measured and calculated OH reactivity agreed, then there was no missing OH reactivity to within the uncertainties for both the measured and the model calculated values. However, if there was missing OH reactivity in the flow tube, then the missing OH reactivity in the atmosphere may be different because the temperature dependence of its reaction rate coefficients is unknown. Fortunately, the focus of this study is in and just above the MBL where the flow tube pressures and temperatures are nearly identical to atmospheric temperatures and pressures. The OH reactivity calculated from the model output at the flow tube pressure and temperature is within ±10% of that calculated at ambient conditions. Thus, the missing OH reactivity calculated at flow tube temperature and pressure is assumed to be equal the atmospheric missing OH reactivity.

If missing OH reactivity is found, a likely source is unknown VOCs or OVOCs, which we will call X. The abundance of X was determined from the missing OH reactivity by Eq. (5).

$$X = \frac{mOHR}{k_{X+OH}} \frac{10^9}{M} \quad (5)$$

where X is the missing chemical species (ppbv), mOHR is the missing OH reactivity, k_{X+OH} is the reaction rate coefficient for the reaction $X + OH \rightarrow$ products, and M is the air number concentration. We assume that $k_{X+OH} = 10^{-10}$ cm^3 s^{-1}, which gives X a lifetime of an hour. For these assumptions, an X abundance of 400 pptv corresponds to a missing OH reactivity of 1 s^{-1}. This arbitrary rate coefficient approximates a rate coefficient for a reaction of a sesquiterpene with OH. If X is an alkane or alkene that has a lower reaction rate coefficient, then the required X abundance would be larger.

Simple X oxidation chemistry was added to the photochemical mechanism to test the impact of X on the modeled OH and HO_2. This assumed chemistry is provided in Table 3. XO_2 is used to designate the peroxy radical formed from X. Rate coefficients for CH_3O_2 and CH_3OOH were assumed to apply to XO_2 and XOOH. Case 1 assumes that no OH is regenerated in the oxidation sequence for X, while case 2 assumes that OH is regenerated for every oxidation sequence of X.

2.5 Correlation Analysis

If missing OH reactivity persists after the background is subtracted from the OH reactivity measurements and a comparison is made to the model calculated OH reactivity, then a correlation analysis might determine its causes, which could then be further investigated. Linear regressions were found for missing OH reactivity and every measured and model-calculated chemical species and meteorological parameter. Model-calculated chemical species with abundances less than 1 pptv were not included in the regressions. Correlations were performed on the first three ATom phases individually and the first three ATom phases combined.

https://doi.org/10.5194/acp-2019-866
Preprint. Discussion started: 16 October 2019


Atmospheric Chemistry and Physics Discussions

To reduce the noise in the missing OH reactivity values prior to doing any correlation analysis, the 1-minute summed missing OH reactivity values were averaged into "per-dip" bins and "per-flight" bins. The standard deviation of the 1-minute measurements within each dip was typically 0.5 s^{-1}, while the standard deviation of the per-dip measurements in a flight was 0.25 s^{-1}. Each per-dip bin is a single value representing an average of the missing OH reactivity as the DC-8 flew a level leg at 200 m. These legs were all in the MBL because its height was greater than 200 m. The MBL height is the altitude below which the potential temperature is constant. Each per-flight bin is the average of each flight's per-dip set. A per-dip bin occurred roughly every hour of flight and is an average of ~5 minutes of missing OH reactivity values. Each per-flight bin spanned only a few degrees of latitude near the poles but as much as 50° of latitude in the tropics. Only the points taken while flying over the ocean were included in the per-dip and per-flight averaging as dips over land sampled terrestrial or ice emissions and not ocean emissions.

Individual measured or model calculated meteorological parameters or chemical species passed a preliminary correlation threshold for missing OH reactivity if the sign of each regression was the same for ATom1, ATom2, and ATom3. Correlations that passed this preliminary filter had their R^2 values averaged between each phase individually and grouped together. Some extreme outlier points were removed before correlations were calculated. The averaged correlation coefficients were then tallied and ranked from greatest to least R^2. The top 10% of these correlations for both the per-dip and per-flight averages were combined into one list. The same multi-step technique was performed on all the chemical species and meteorological parameters as they were correlated with latitude as well, under a similar breakdown for Northern, Southern, Eastern and Western hemispheres. Both lists were then combined into a single list and the strongest of these correlations were reported.

3 Results

The focus of these results is the OH reactivity measurements in and just above the MBL. However, the OH reactivity measurements are shown for the entire range of altitudes, even though the high-altitude (>10 km) OH reactivity values were set to the model calculated OH reactivity that was corrected to the OHR flow tube pressure and temperature.

The average calculated global OH reactivity at the lowest altitudes is about an order of magnitude less than the average OH reactivity in cities or forests (Yang et al., 2016). Model-calculated OH reactivity is less than 2 s^{-1} averaged over all latitudes and seasons (Fig. 4). In different seasons and regions, this calculated OH reactivity consists of CO (30-40%), CH_4 (19-24%), methyl hydroperoxide (MHP) (5-16%), aldehydes (11-12%), H_2 (6-7%), O_3 (2-5%), and HO_2 (2-6%), with the remaining reactants totaling less than 10%. The ordering of these reactants is similar to that of Mao et al. (2009), although in their work the calculated OH reactivity due to CO was about 60% and CH_4 about 15%, and all OVOCs about 16%. Part of this

https://doi.org/10.5194/acp-2019-866
Preprint. Discussion started: 16 October 2019


Atmospheric Chemistry and Physics Discussions

difference can be ascribed to more OVOC measurements in ATom and the greater CO abundances in the Northern hemisphere where INTEX-B occurred.

3.1 Global OH Reactivity Over Oceans

The median measured OH reactivity equals the median model-calculated OH reactivity to within ±1σ statistical uncertainty until below 2-4 km, where it becomes greater than the median model-calculated OH reactivity (Fig. 4). The median missing OH reactivity becomes greater than 0 below 2-4 km, depending on the ATom phase, reaching median values between 0.2 and 0.8 s^{-1} in the marine boundary layer (MBL) for ATom1 through ATom3. In some locations, primarily the northern and tropical Pacific Ocean, missing OH reactivity was 1-2 s^{-1}, and even larger on a few occasions.

3.2 Missing OH Reactivity: Statistical Evidence

For missing OH reactivity to be meaningful, some missing OH reactivity points must be much greater than the statistical spread of the OH reactivity measurements. Missing OH reactivity is not measured above 8 km because we assumed no measurable OH reactivity was there in order to identify the internal instrument contamination for each flight. However, these data provide insight into the measurement precision (Fig. 5). Missing OH reactivity is shown for ATom1, ATom2, and ATom3. The dotted black bands represent ±2σ standard deviation for data averaged into 0.5 km altitude bins. About 95% of all points above 4 km are within that phase's 2σ uncertainty bands, which is consistent with a statistically normal distribution.

Quantile-quantile plots provide a visual description of the differences in the distributions of missing OH reactivity values above 8 km and below 4 km, representing the top third (8-12 km) and bottom third (0-4 km) of the sampled troposphere (Fig. 6). If these values were purely normal distributions, as would be expected from a missing OH reactivity created solely by the instrument uncertainty, then they would lie along the red dashed lines. Values higher than the red dashed line indicate that the number of missing OH reactivity values in that part of the distribution is much greater than would be expected for a normal distribution. The missing OH reactivity values measured below 4 km altitude lie along the red dashed line, which passes through (0.0, 0.0), indicating that the median value is 0 s^{-1} and the values follow the normal distribution. However, while more than 90% of the missing OH reactivity values below 4 km follow the normal distribution, there are many missing OH reactivity values that fall above those predicted by a strictly normal distribution. This deviation from a normal distribution indicates that the missing OH reactivity exceeds the statistical error range.

A Student t-test also determines whether the missing OH reactivity from the lowest 4 km is statistically consistent with the normally distributed points above 4 km. For each campaign, the calculated p-values are below 10^{-5}. As a result, we can reject the null hypothesis that the missing OH reactivity in the lower troposphere comes from the same distribution as those in the upper troposphere. These two tests provide statistical evidence that the observed missing OH reactivity is significant.

https://doi.org/10.5194/acp-2019-866
Preprint. Discussion started: 16 October 2019

Atmospheric Chemistry and Physics Discussions

3.3 Correlation of Missing OH Reactivity with Other Factors

From the correlation analysis described in Section 2.5, only a few factors stand out as being related to missing OH reactivity. The first is latitude. Figure 7 illustrates this correlation by plotting the missing OH reactivity as colored circles along the same flight tracks and dip locations as in Fig. 1. Missing OH reactivity is higher in the tropics and mid-latitudes and lower near the poles, in addition to having slightly increased values in the summer hemisphere. Most missing OH reactivity is less than 2 s^{-1} across all latitudes and seasons. The latitudinal dependence implies that air or sea temperature or other latitude-dependent factors contribute to missing OH reactivity. Further, Fig. 7 also shows evidence that the missing OH reactivity in the northern Pacific is greater than that in any other hemisphere.

A special note should be made regarding the northern Pacific data for ATom2. One flight (Anchorage, Alaska to Kailua-Kona, Hawai'i) accounts for every missing OH reactivity value greater than ~2 s^{-1}. These points are anomalous in the context of all ATom OH reactivity measurements, and they do not correlate with the modeled influence from fires, convection, land, or the stratosphere. While present on some figures for completeness, they were not included in the correlation analysis.

Following the procedure given in Section 2.5, the main correlations that stand out are butanal (C_3H_7CHO), dimethyl sulfide (DMS, CH_3SCH_3), formaldehyde (HCHO), and sea surface temperature (SST), as shown in Fig. 8. A number of modeled pptv-level butanal products also correlate with missing OH reactivity. Interestingly, missing OH reactivity correlates only weakly with acetaldehyde and chlorophyll. SST and chlorophyll data come from NASA Earth Observations (2019). These correlations suggest that the missing OH reactivity comes for an unknown VOC or OVOC that has HCHO and butanal as products and is co-emitted with DMS. The correlation with SST suggests an ocean source, as a higher temperature implies more emissions. Either biological activity of phytoplankton in the sea surface microlayer (Brooks and Thornton, 2017; Lana et al., 2011) or abiotic sea surface interfacial photochemistry (Brüggemann et al., 2018) could be the source of these VOCs and OVOCs.

3.4 Comparison to INTEX-B

HCHO is a good indicator for VOC photochemistry because it is an oxidation product for many VOCs. Thus, HCHO should correlate with missing OH reactivity. The ATom missing OH reactivity at the per-dip time resolution is compared to Mao's missing OH reactivity below 2 km for times when NO is less than 100 pptv (Fig. 9). We use the per-dip time resolution of ~5 minutes in this comparison rather than per-flight to better align with the time resolution in Mao et al. (2009) of 3.5 minutes. While the overall INTEX-B correlation coefficient between missing OH reactivity and HCHO ($R^2 = 0.58$) is greater than the one found for ATom ($R^2 = 0.35$), in the range of ATom HCHO (100 pptv – 500 pptv), the ATom case is better correlated. The ATom results corroborate the Mao et al. correlation of missing OH reactivity with HCHO.

https://doi.org/10.5194/acp-2019-866
Preprint. Discussion started: 16 October 2019


Atmospheric Chemistry and Physics Discussions

The linear fit of the missing OH reactivity against HCHO data from Mao et al. (2009) is given as the solid red line in Fig. 9. If instead the pressure-dependent background is used, then the resulting missing OH reactivity against HCHO follows the dashed red line. With the INTEX-B background uncertainty at ±0.5 s^{-1} and ATom background uncertainty at ±0.4 s^{-1}, both at the 1σ confidence level, the linear fits for missing OH reactivity against HCHO in ATom and INTEX-B agree to within combined uncertainties. Thus, the adjusted missing OH reactivity found in INTEX-B is consistent with the missing OH reactivity found in the ATom phases over the northern Pacific Ocean.

4 Discussion

Mao et al. (2009) calculated HO_2/OH assuming that the cycling between OH and HO_2 was much greater than HO_x production. That assumption is not valid for ATom because the low NO and OH reactivity values reduce the recycling to rates comparable to HO_x production. On the other hand, by adding simple X photochemistry to the MCMv331 mechanism, as discussed in Section 2.3, it is possible to determine if the measured OH and HO_2 are consistent with observed missing OH reactivity. For case 1 in which there is no OH produced in the X oxidation sequence, the modeled OH and HO_2 become substantially less than observed at altitudes below 6 km. On the other hand, if XO_2 and its products autoxidize to produce OH (Crounse et al., 2013), then the modeled OH and to a lesser extent HO_2 become greater than observed. The optimum agreement between observed and modeled OH and HO_2 would require a partial recycling of OH, but without knowing the identity of X, it is not possible to know the fraction of OH that should be recycled in the chemical mechanism. Thus, this analysis neither supports nor refutes the missing OH reactivity measurements.

Several recent studies provide evidence for an unknown VOC or OVOC emitted into the atmosphere from the ocean. Oceanic sources have also been proposed for butanes and pentanes in some regions (Pozzer et al., 2010) and for methanol (Read et al., 2012). Measurements of biogenic VOCs in coastal waters found monoterpenes, C12-C15 n-alkenes, and several higher aldehydes that could contribute to enhanced OH reactivity (Tokarek et al., 2019).

Unexpectedly large abundances of acetaldehyde (CH_3CHO) have been observed in the marine boundary layer and the free troposphere (Singh et al., 2004; Millet et al., 2010; Read et al., 2012; Nicely et al., 2016; Wang et al., 2019) and the ocean is suspected to be the source. While earlier measurements may have been compromised with interferences, recent measurements of unexpectedly high acetaldehyde abundances are supported by unexpectedly large abundances of peroxyacetic acid, which is produced almost exclusively through acetaldehyde oxidation (Wang et al., 2019). Wang et al. observed that the ocean effects on acetaldehyde were confined primarily to the MBL and were able to approximately model the vertical distribution by using direct ocean emissions of acetaldehyde. However, it is possible that some of the observed acetaldehyde was produced by rapid oxidation of VOCs or OVOCs emitted from the ocean.

https://doi.org/10.5194/acp-2019-866
Preprint. Discussion started: 16 October 2019

The missing OH reactivity is primarily in the MBL, but often extends upward to as high as 2 km to 4 km in some dips. Above 4 km, the OH reactivity measurements are too near their LOD and thus too noisy to know if OH reactivity and acetaldehyde decrease the same way with altitude, but it is possible that they do. A similar decrease with altitude would imply that the unknown reactant lives long enough to be distributed throughout the free troposphere. If, on the other hand, the missing OH reactivity is only in and just above the planetary boundary layer, then the unknown reactant could have a much shorter lifetime. The lack of correlation between missing OH reactivity and acetaldehyde in the MBL suggests that the unknown reactant responsible for the missing OH reactivity is not necessarily connected only to an ocean source of acetaldehyde.

From Eq. (5) and the measured missing OH reactivity, the abundance of the chemical species X would typically be a few tenths of a ppbv, assuming that X is a sequiterpene with a typical reaction rate coefficient of $1x10^{-10}$ cm^3 s^{-1}. The median value for X is 0.26 ± 0.23 ppbv for the per-dip bins. If X is an alkane with a typical reaction rate coefficient of $2.3x10^{-12}$ cm^3 s^{-1}, then its mixing ratio would need to be more than 10 ppbv.

The lifetime of the unknown VOC is important because it determines the source strength necessary to maintain the measured missing OH reactivity. For instance, if the unknown VOC is an alkane with a reaction rate coefficient with OH of $2.3x10^{-12}$ cm^3 s^{-1}, then an unlikely large oceanic source of 360 Tg C yr^{-1} would be necessary (Travis et al., 2019). However, if the unknown VOC is an alkene, such as a sesquiterpene, then the reaction rate coefficient with OH would be ~$1x10^{-10}$ cm^3 s^{-1} and the required oceanic source would be a more reasonable 8 Tg C yr^{-1}.

5 Conclusion

Measured OH reactivity significantly exceeds calculated OH reactivity in the marine boundary layer during ATom. This missing OH is most prominent over the northern and tropical Pacific Ocean where it had median values of 0.2-0.8 s-1 for the different ATom phases, but rose to more than 1-2 s^{-1} in some locations. These higher values correspond to ~0.5 ppbv of a fast-reacting VOC, such as a sesquiterpene. The correlation of missing OH reactivity with formaldehyde, butanal, dimethyl sulfide, and sea surface temperature and the requirements for a smaller unknown reactive gas abundance and ocean source strength suggest that an ocean source of short-lived reactive gases, possibly VOCs or OVOCs, is responsible. This missing OH reactivity is qualitatively consistent with the observed unexpectedly large abundances of acetaldehyde, peroxyactic acid, and other oxygenated VOCs. They may share the same cause. Finding this cause will require focused studies of detailed atmospheric composition in regions where missing OH reactivity and acetaldehyde excess are greatest.

Data and Model Availability

The data and model used in this paper are publicly available:

- data: https://doi.org/10.3334/ORNLDAAC/1581

https://doi.org/10.5194/acp-2019-866
Preprint. Discussion started: 16 October 2019

Atmospheric Chemistry and Physics Discussions

- model framework: https://github.com/airchem/F0AM
- MCMv331 chemical mechanism: http://mcm.leeds.ac.uk/MCM/

Author Contribution

ABT, DOM, and WHB made the OH, HO_2, and OH reactivity measurements, performed the model runs, analyzed the data, and wrote the manuscript. GMW provided support of the use of the F0AM model framework used for the model runs. WHB, DOM, ABT, HMA, DRB, TPB, RC, JDC, BCD, GSD, JPD, JWE, SRH, TFH, RAH, EH, MJK, KM, FLM, JMN, JP, TBR, JMS, CS., APT, CT, KU, POW, GMW provided ATom measurements used for the modeling and reviewed and edited the manuscript.

Competing Interests

The authors declare no financial or affiliation conflicts-of-interest.

Funding

This study was supported by the NASA grant NNX15AG59A. This material is based upon work supported by the National Center for Atmospheric Research, which is a major facility sponsored by the National Science Foundation under Cooperative Agreement No. 1852977.

Acknowledgements

The authors thank the NASA ATom management team, pilots, logistical support team, aircraft operations team, and fellow scientists.

References

Apel, E. C., Hornbrook, R. S., Hills, A. J., Blake, N. J., Barth, M. C., Weinheimer, A., Cantrell, C., Rutledge, S. A., Basarab, B., Crawford, J., Diskin, G., Homeyer, C. R., Campos, T., Flocke, F., Fried, A., Blake, D. R., Brune, W., Pollack, I., Peischl, J., Ryerson, T., Wennberg, P. O., Crounse, J. D., Wisthaler, A., Mikoviny, T., Huey, G., Heikes, B., O'Sullivan, D., and Riemer, D. D.: Upper tropospheric ozone production from lightning NOx-impacted convection: Smoke ingestion case study from the DC3 campaign, *Journal of Geophysical Research: Atmospheres*, doi:10.1002/2014JD022121,2015.

Assaf, E., Sheps, L., Whalley, L., Heard, D., Tomas, A., Schoemaecker, C., Fittschen, C.: The Reaction between CH_3O_2 and OH Radicals: Product Yields and Atmospheric Implications, Environ. Sci. Technol., 51, 2170−2177, DOI: 10.1021/acs.est.6b06265, 2017.

ATom: Measurements and modeling results from the NASA Atmospheric Tomography Mission, available at: https://espoarchive. nasa.gov/archive/browse/atom (last access: 9 August 2019), 2016.

Brooks S.D, Thornton D.C.O: Marine Aerosols and Clouds, Annual Review of Marine Science, 10, 289-313, https://doi.org/10.1146/annurev-marine-121916-063148, 2017.

Brüggemann, M. Hayeck, N., George, C.: Interfacial photochemistry at the ocean surface is a global source of organic vapors and aerosols, Nature Communications, 9, Article number: 3222, 2018.

Cazorla, M., Wolfe, G. M., Bailey, S. A., Swanson, A. K., Arkinson, H. L., and Hanisco, T. F.: A new airborne laser-induced fuorescence instrument for in situ detection of formaldehyde throughout the troposphere and lower stratosphere. Atmos. Meas. Tech., 8, 541-552. doi:194-10.5194/amt-8-541-2015, 2015.

Chan, K. R., Dean-Day, J., Bowen, S. W., and Bui, T. P.:Turbulence measurements by the DC-8 meteorological measurement system. Geophys. Res. Lett., 25, 1355-1358. doi: 10.1029/97GL03590, 1998.

https://doi.org/10.5194/acp-2019-866
Preprint. Discussion started: 16 October 2019

Atmospheric Chemistry and Physics Discussions

Chen, H., Karion, A., Rella, C. W., Winderlich, J., Gerbig, C., Filges, A., Tans, P. P.: Accurate measurements of carbon monoxide in humid air using the cavity ring-down spectroscopy (CRDS) technique. *Atmos. Meas. Tech., 6*, 1031-1040. doi: 10.5194/amt-6-1031-2013, 2013.

Colman, J. J., Swanson, A. L., Meinardi, S., Sive, B. C., Blake, D. R., and Rowland, F. S.: Description of the analysis of a wide range of volatile organic compounds in whole air samples collected during PEM-Tropics A and B. Anal. Chem., 73, 3723-3731. doi: 10.1021/ac010027g, 2001.

Crounse, J. D., McKinney, K. A., Kwan, A. J., and Wennberg, P. O.: Measurement of gas-phase hydroperoxides by chemical ionization mass spectrometry. Anal. Chem., 78, 6726-6732. doi: 10.1021/ac0604235, 2006.

Crounse, J.D.; Nielsen, L.B., Jorgensen, S., Kjaergaard, H.G., and Wennberg, P.O.: Autoxidation of Organic Compounds in the Atmosphere, J. Phys. Chem. Lett., 4, 3513−3520, dx.doi.org/10.1021/jz4019207, 2013.

Di Carlo, P., Brune, W.H., Martinez, M., Harder, H., Lesher, R., Ren, X. R., Thornberry, T., Carroll, M. A., Young, V., Shepson, P. B., Riemer, D. Apel, E., Campbell, C.: Missing OH reactivity in a forest: Evidence for unknown reactive biogenic VOCs, Science, **304**, 722-725, 2004.

Diskin, G. S., Podolske, J. R., Sachse, G. W., and Slate, T. A.: Open path airborne tunable diode laser hygrometer. Diode lasers appl. atmos. sens., 4817, 196, International Society for Optics and Photonics. doi: 225 10.1117/12.453736, 2003.

Fuchs, H., Novelli A., Rolletter M., Hofzumahaus A., Pfannerstill E.Y., Kessel S., Edtbauer A., Williams J., Michoud V., Dusanter S., Locoge N., Zannoni N., Gros V., Truong F., Sarda-Esteve R., Cryer D.R., Brumby C.A., Whalley L.K., Stone D., Seakins P.W., Heard D.E., Schoemaecker C., Blocquet M., Coudert S., Batut S., Fittschen C., Thames A.B., Brune W.H., Ernest C., Harder H., Muller J.B.A., Elste T., Kubistin D., Andres S., Bohn B., Hohaus T., Holland F., Li X., Rohrer F., Kiendler-Scharr A., Tillmann R., Wegener R., Yu Z., Zou Q., Wahner A: Comparison of OH reactivity measurements in the atmospheric simulation chamber SAPHIR, Atmos. Meas. Tech., 10, 4023–4053, https://doi.org/10.5194/amt-10-4023-2017, 2017.

Goldstein, A. H., Galbally, I. E.: Known and unexplored organic constituents in the Earth's Atmosphere, Env. Sci. Tech., 41(5), 1514–1521, doi:10.1021/es072476p, 2007.Kaiser, J., Skog, K. M., Baumann, K., Bertman, S. B., Brown, S. B., Brune, W. H., Crounse, J. D., de Gouw, J. A., Edgerton, E. S., Feiner, P. A., Goldstein, A. H., Koss, A., Misztal, P. K., Nguyen, T. B., Olson, K. F., St. Clair, J. M., Teng, A. P., Toma, S., Wennberg, P. O., Wild, R. J., Zhang, L. and Keutsch, F. N.: Speciation of OH reactivity above the canopy of an isoprene-dominated forest, Atmos. Chem. Phys., 16(14), 9349–9359, doi:10.5194/acp-16-9349-2016, 2016.

Jenkin, M. E., Saunders, S. M., Wagner, V., and Pilling, M. J.: Protocol for the development of the Master Chemical Mechanism, MCM v3 (Part B): tropospheric degradation of aromatic volatile organic compounds, Atmos. Chem. Phys., 3, 181-193, https://doi.org/10.5194/acp-3-181-2003, 2003.

Kaiser, J., Skog, K. M., Baumann, K., Bertman, S. B., Brown, S. B., Brune, W. H., Crounse, J. D., De Gouw, J. A., Edgerton, E. S., Feiner, P. A., Goldstein, A. H., Koss, A., Misztal, P. K., Nguyen, T. B., Olson, K. F., St Clair, J. M., Teng, A. P., Toma, S., Wennberg, P. O., Wild, R. J., Zhang, L. and Keutsch, F. N.: Speciation of OH reactivity above the canopy of an isoprene dominated forest, Atmos. Chem. Phys., doi:10.5194/acp-16-9349-2016, 2016.

Kovacs, T. A. and Brune, W. H.: Total OH loss rate measurement, J. Atmos. Chem., 39(2), 105–122, doi:10.1023/A:1010614113786, 2001.

Kovacs, T.A., Brune, W. H., Harder, H., Martinez, M., Simpas, J. B., Frost, G. J., Williams, E., Jobson, T., Stroud, C., Young, V., Fried, A., Wert, B.: Direct measurements of urban OH reactivity during Nashville SOS in summer 1999, J. Environ. Monitoring, 5 (1), 68-74, 2003.

Lana A., Bell T.G., Simó R., Vallina S.M., Ballabrera-Poy J., Kettle A. J., Dachs J., Bopp L., Saltzman E.S., Stefels J., Johnson J.E., Liss P.S.: An updated climatology of surface dimethylsulfide concentrations and ecampaign fluxes in the global ocean, Global Biogeochemical Cycles, 25, GB1004, https://doi.org/10.1029/2010GB003850, 2011.

Lambe, A.T., Ahern, A.T., Williams, L.R., Slowik, J. G., Wong, J. P. S., Abbatt, J. P. D., Brune, W. H., Ng, N. L., Wright, J. P., Croasdale, D. R., Worsnop, D. R., Davidovits, P., Onasch, T. B.: Characterization of aerosol photooxidation flow reactors: heterogeneous oxidation, secondary organic aerosol formation and cloud condensation nuclei activity measurements, Atmospheric Measurement Techniques, 4, 445-461, 10.5194/amt-4-445-2011, 2011.

Maasakkers, J. D., Jacob, D. J., Sulprizio, M. P., Scarpelli, T. R., Nesser, H., Sheng, J.-X., Zhang, Y., Hersher, M., Bloom, A. A., Bowman, K. W., Worden, J. R., Janssens-Maenhout, G., and Parker, R. J.: Global distribution of methane

emissions, ecampaign trends, and OH concentrations and trends inferred from an inversion of GOSAT satellite data for 2010–2015, Atmos. Chem. Phys., 19, 7859-7881, https://doi.org/10.5194/acp-19-7859-2019, 2019.

Mao J., Ren, X., Brune, W. H., Olson, J. R., Crawford, J. H., Fried, A., Huey, L. G., Cohen, R. C., Heikes, B., Singh, H. B., Blake, D. R., Sachse, G. W., Diskin, G. S., Hall, S. R., and Shetter, R. E.: Airborne measurement of OH reactivity during INTEX-B, Atmospheric Chemistry and Physics, 9, 163-173, 2009.

Millet, D. B., Guenther, A., Siegel, D. A., Nelson, N. B., Singh, H. B., de Gouw, J. A., et al.: Global atmospheric budget of acetaldehyde: 3-D model analysis and constraints from in-situ and satellite observations. Atmospheric Chemistry and Physics, 10(7), 3405–3425. https://doi.org/10.5194/acp-10-3405-2010, 2010.

Naik, V., Voulgarakis, A., Fiore, A. M., Horowitz, L. W., Lamarque, J.-F., Lin, M., Prather, M. J., Young, P. J., Bergmann, D., Cameron-Smith, P. J., Cionni, I., Collins, W. J., Dalsøren, S. B., Doherty, R., Eyring, V., Faluvegi, G., Folberth, G. A., Josse, B., Lee, Y. H., MacKenzie, I. A., Nagashima, T., van Noije, T. P. C., Plummer, D. A., Righi, M., Rumbold, S. T., Skeie, R., Shindell, D. T., Stevenson, D. S., Strode, S., Sudo, K., Szopa, S., and Zeng, G.: Preindustrial to present-day changes in tropospheric hydroxyl radical and methane lifetime from the Atmospheric Chemistry and Climate Model Intercomparison Project (ACCMIP), Atmos. Chem. Phys., 13, 5277-5298, https://doi.org/10.5194/acp-13-5277-2013, 2013.

NASA Earth Observations: https:// https://neo.sci.gsfc.nasa.gov/, last access: 5 August 2019.

Nicely, J. M., Anderson, D. C., Canty, T. P., Salawitch, R. J., Wolfe, G .M., et al.: An observationally constrained evaluation of the oxidative capacity in the tropical western Pacific troposphere,, J. Geophys. Res.Atmos.,121, 7461–7488, doi:10.1002/2016JD025067, 2016.

Neuman, J. A., Trainer, M., Brown, S. S., Min, K.-E., Nowak, J. B., Parrish, D. D., and Veres, P. R.: HONO emission and production determined from airborne measurements over the Southeast U.S., J. Geophys. Res. Atmos., 121, 9237-9250. doi: 10.1002/2016JD025197, 2016.

Nölscher, A. C., Williams, J., Sinha, V., Custer, T., Song, W., Johnson, A. M., Axinte, R., Bozem, H., Fischer, H., Pouvesle, N., Phillips, G., Crowley, J. N., Rantala, P., Rinne, J., Kulmala, M., Gonzales, D., Valverde-Canossa, J., Vogel, A., Hoffmann, T., Ouwersloot, H. G., Vilà-Guerau de Arellano, J. and Lelieveld, J.: Summertime total OH reactivity measurements from boreal forest during HUMPPA-COPEC 2010, Atmos. Chem. Phys., 12(17), 8257–8270, doi:10.5194/acp-12-8257-2012, 2012.

Nölscher, A. C., Yañez-Serrano, A. M., Wolff, S., de Araujo, A. C., Lavrič, J. V., Kesselmeier, J. and Williams, J.: Unexpected seasonality in quantity and composition of Amazon rainforest air reactivity, Nature Communications, 7(1), doi:10.1038/ncomms10383, 2016.

Pfannerstill, E. Y., Wang, N., Edtbauer, A., Bourtsoukidis, E., Crowley, J. N., Dienhart, D., Eger, P. G., Ernle, L., Fischer, H., Hottmann, B., Paris, J.-D., Stönner, C., Tadic, I., Walter, D., Lelieveld, J., and Williams, J.: Shipborne measurements of total OH reactivity around the Arabian Peninsula and its role in ozone chemistry, Atmos. Chem. Phys. Discuss., https://doi.org/10.5194/acp-2019-416, in review, 2019.

Pozzer, A., Pollmann, J., Taraborrelli, D., Jockel, P., Helmig, D., Tans, P., Hueber, J., Lelieveld, J.: Observed and simulated global distribution and budget of atmospheric C2−C5 alkanes. Atmos. Chem. Phys., 10, 4403−4422, 2010.

Prather, M. J., Holmes, C. D., and Hsu, J.: Reactive greenhouse gas scenarios: Systematic explorationof uncertainties and the role of atmospheric chemistry, Geophys.Res. Lett.,39, L09803, doi:10.1029/2012GL051440, 2012.

Read, K. A., Carpenter, L. J., Arnold, S. R., Beal, R., Nightingale, P. D., Hopkins, J. R., Lewis, A. C., Lee, J. D., Mendes, L., Pickering, S. J.: Multiannual Observations of Acetone, Methanol, and Acetaldehyde in Remote Tropical Atlantic Air: Implications for Atmospheric OVOC Budgets and Oxidative Capacity, Environ, Sci. Tech., 46, 11028−11039, dx.doi.org/10.1021/es302082p, 2012.

Ryerson, T. B., Williams, E. J., and Fehsenfeld, F. C.: An efficient photolysis system for fast response NO_2 measurements. J. Geophys. Res. Atmos., 105, 26447-26461. doi: 10.1029/2000JD900389, 2000.

Santoni, G. W., Daube, B. C., Kort, E. A., Jimenez, R., Park, S., Pittman, J. V., Wofsy, S. C.: Evaluation of the airborne quantum cascade laser spectrometer (QCLS) measurements of the carbon and greenhouse gas suite - CO_2, CH_4, N_2O, and CO - during the CalNex and HIPPO Campaigns, Atmos. Meas. Tech., 7, 1509-1526. doi: 10.5194/amt-7-1509-2014, 2014.

https://doi.org/10.5194/acp-2019-866
Preprint. Discussion started: 16 October 2019

Atmospheric Chemistry and Physics Discussions

Saunders, S. M., Jenkin, M. E., Derwent, R. G., and Pilling, M. J.: Protocol for the development of the Master Chemical Mechanism, MCM v3 (Part A): tropospheric degradation of non-aromatic volatile organic compounds, Atmos. Chem. Phys., 3, 161-180, https://doi.org/10.5194/acp-3-161-2003, 2003.

Shetter, R. E. and Mueller, M.: Photolysis frequency measurements using actinic flux spectroradiometry during the PEM-Tropics mission: Instrumentation description and some results, J. Geophys. Res. Atmos., 104, 5647-5661. doi: 10.1029/98JD01381, 1999.

Singh H.B., Salas L.J., Chatfield R.B., Czech, E., Fried A., Walega J., Evans M.J., Field B.D., Jacob D.J., Blake D., Heikes B., Talbot R., Sachse G., Crawford J. H., Avery M.A., Sandholm S., Fuelberg H.: Analysis of the atmospheric distribution, sources, and sinks of oxygenated volatile organic chemicals based on measurements over the Pacific during TRACE-P, Journal of Geophysical Research: 109, D15S07, https://doi.org/10.1029/2003JD003883, 2004.

Tokarek, T. W., Brownsey, D. K., Jordan, N., Garner, N. M., Ye, C. Z., Osthoff, H. D.: Emissions of C9 – C16 hydrocarbons from kelp species on Vancouver Island: Alaria marginata (winged kelp) and Nereocystis luetkeana (bull kelp) as an atmospheric source of limonene, Atmos. Environ. X, 2, Article 100007, 2019.

Wang, S., Hornbrook, R. S., Hills, A., Emmons, L. K., Tilmes, S., Lamarque, J.-F., et al.: Atmospheric acetaldehyde: Importance of air-sea exchange and a missing source in the remote troposphere. Geophysical Research Letters, 46, 5601–5613. https://doi.org/10.1029/2019GL082034, 2019.

Wolfe, G.M, Marvin, M.R., Roberts, S.J., Travis, K.R., and Liao, J.: The Framework for 0-D Atmospheric Modeling (F0AM) v3.1, Geosci. Model Dev., 9, 3309-3319, doi: 10.5194/gmd-9-3309-2016, 2016.

Yang, Y, Shao, M., Wang, X., Noelscher, A.C., Kessel, S., Guenther, A., Williams, J.: Towards a quantitative understanding of total OH reactivity: A review, Atmos. Environ., 143, 147-161, 2016.

Zannoni, N., Gros, V., Lanza, M., Sarda, R., Bonsang, B., Kalogridis, C., Preunkert, S., Legrand, M., Jambert, C., Boissard,C., Lathiere, J.: OH reactivity and concentrations of biogenic volatile organic compounds in a Mediterranean forest of downy oak trees, Atmos. Chem. Phys., 16(3), 1619–1636, doi:10.5194/acp-16-1619-2016, 2016.

https://doi.org/10.5194/acp-2019-866
Preprint. Discussion started: 16 October 2019

Atmospheric Chemistry and Physics Discussions

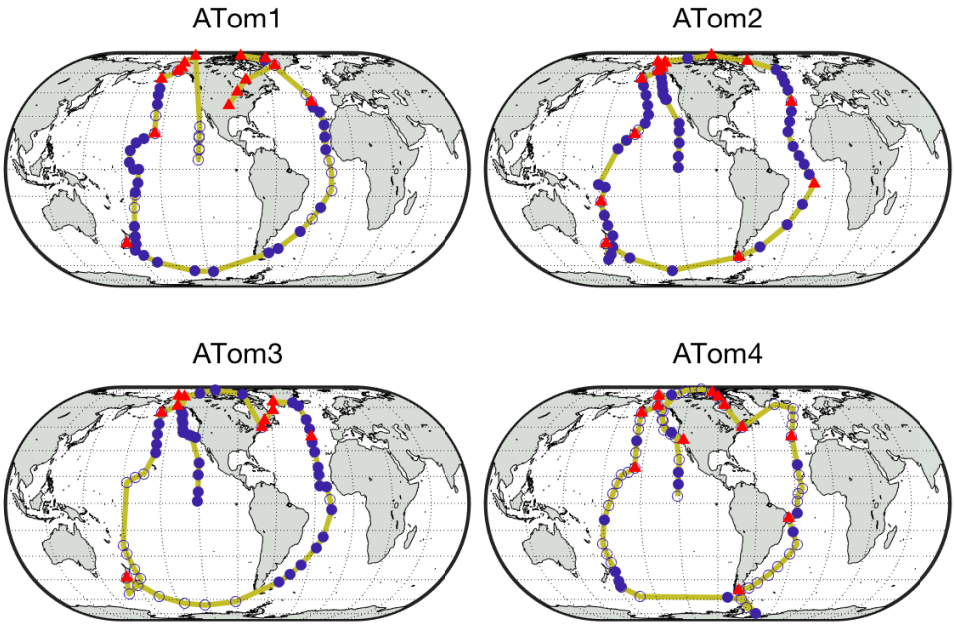

590 **Figure 1: Global ATom tracks (yellow lines) with indicators for the periods during which the DC-8 dipped into the boundary layer. Filled blue circles indicate points used for analysis; filled red triangles indicate dips when over land; unfilled blue circles indicate dips not used for analysis due to instrument calibrations or downtime.**

https://doi.org/10.5194/acp-2019-866
Preprint. Discussion started: 16 October 2019

Atmospheric Chemistry and Physics Discussions

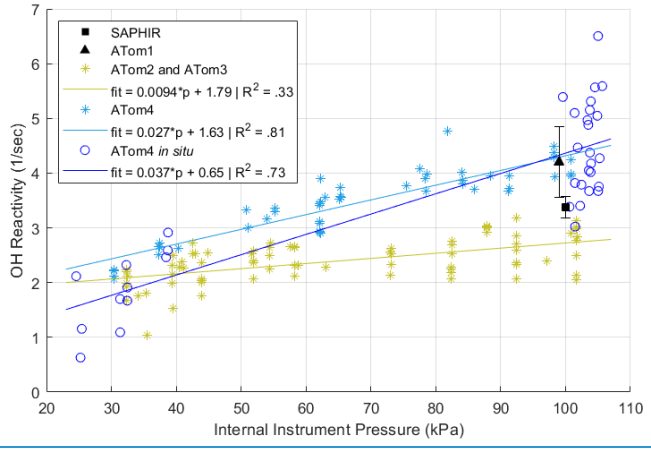

595

Figure 2. Laboratory and in situ calibrations of OHR background decay over 1-minute sums. Black points represent data for which the background calibrations were done only at ~100 kPa in 2015 and 2016. SAPHIR refers to the OH reactivity intercomparison study (Fuchs et al., 2017). Yellow coloring indicates data collected in 2017; blue colorings indicate data collected in 2018. Stars indicate laboratory calibrations; circles indicate in situ data points.

600

https://doi.org/10.5194/acp-2019-866
Preprint. Discussion started: 16 October 2019

Atmospheric Chemistry and Physics Discussions

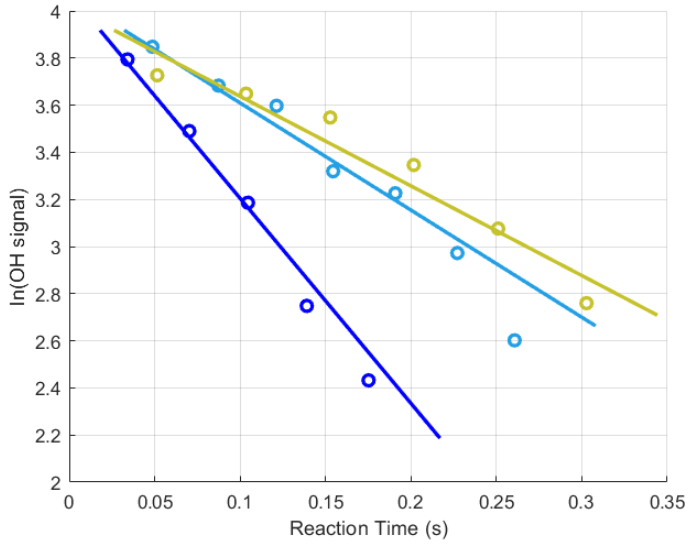

Figure 3: Three in-flight decays for 1-minute sums of the OH signals. Decays were measured in the marine boundary layer and the individual 5 Hz data were binned by reaction times for clarity. When $k_{background}$ is subtracted from the decays, their values become ~5 s^{-1} (blue), ~3 s^{-1} (teal), and ~2 (yellow) s^{-1}.

https://doi.org/10.5194/acp-2019-866
Preprint. Discussion started: 16 October 2019

Atmospheric Chemistry and Physics Discussions

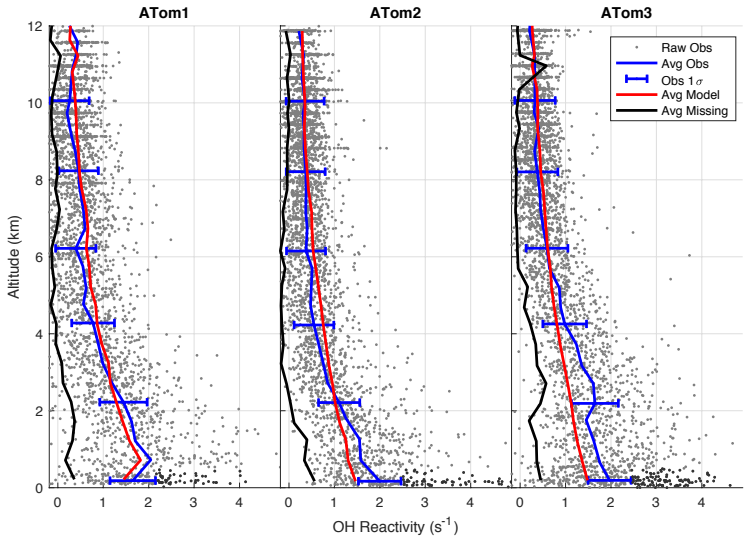

610 **Figure 4. OH reactivity versus altitude for each ATom campaign. The grey points represent each 1-minute measured OHR value with the instrument offset and internal contamination removed. The median OH reactivity of 500m altitude bins is shown for measured OH reactivity (blue line, with 1σ error bars), for model-calculated OH reactivity (red line), and for missing OH reactivity (black line). Darker grey points indicate OH reactivity values greater than the 1σ uncertainty in the MBL.**

https://doi.org/10.5194/acp-2019-866
Preprint. Discussion started: 16 October 2019

Atmospheric Chemistry and Physics Discussions

615

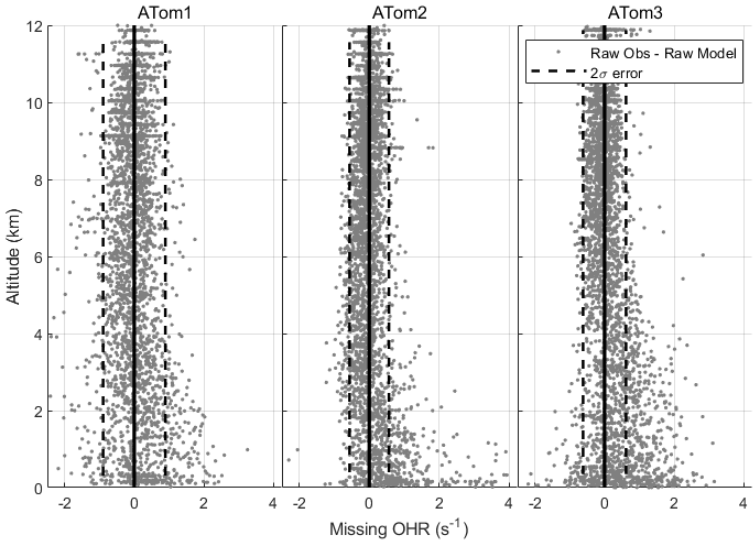

Figure 5: Missing OH reactivity against altitude for ATom1, ATom2, and ATom3. Grey dots are the OH reactivity calculated by the model subtracted from the measured OH reactivity. Dotted black lines represent ±2σ uncertainty derived from a median of the missing OH reactivity values greater than 4 km.

620

https://doi.org/10.5194/acp-2019-866
Preprint. Discussion started: 16 October 2019

Atmospheric Chemistry and Physics Discussions

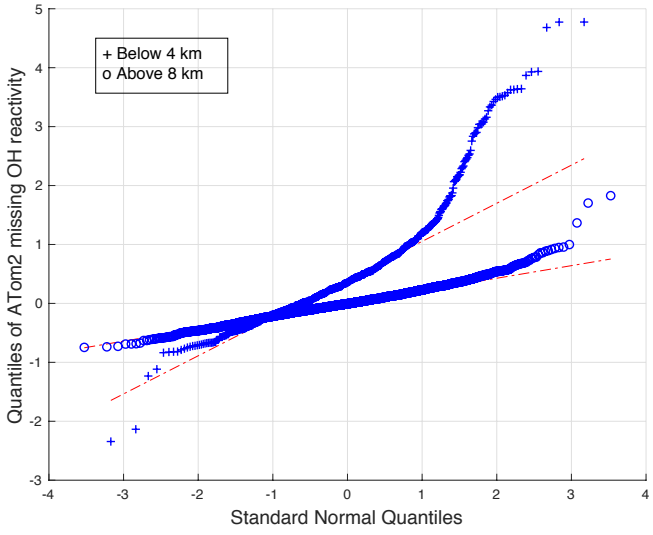

Figure 6: ATom2 quantile-quantile plot for 1-minute missing OH reactivity values above 8 km (circles) and below 4 km (plusses) versus a normal distribution with a mean of 0 and a standard deviation of 1. The values lie along the red dashed lines if the missing OH reactivity values are normally distributed. This q-q plot is for ATom2; the q-q plots for ATom1 and ATom3 have similar characteristics.

https://doi.org/10.5194/acp-2019-866
Preprint. Discussion started: 16 October 2019

Atmospheric Chemistry and Physics Discussions

630

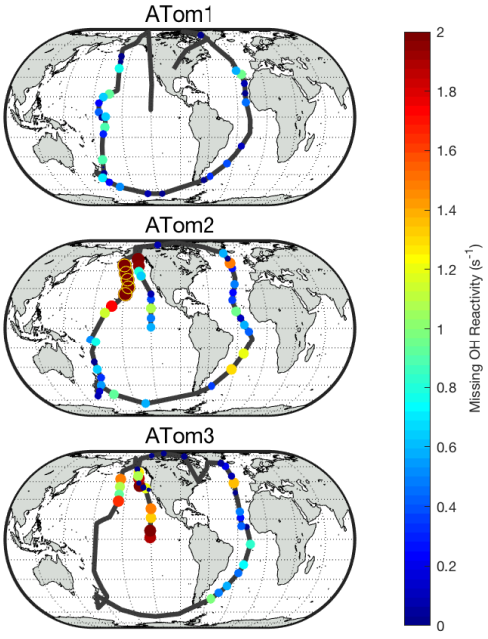

Figure 7. Global missing OH reactivity forATom1, ATom2, and ATom3 at the per-dip time resolution. The black lines trace the flight path during each phase, identical to the yellow tracks in Figure 1. Color and size indicate the missing OH reactivity (larger and red being greater values), while the yellow open circles indicate values in ATom2 above 2 s^{-1} that were not included in the correlation analysis. Each missing OH reactivity value has a 1σ error of ~±0.5 s^{-1} across each ATom phase.

635

https://doi.org/10.5194/acp-2019-866
Preprint. Discussion started: 16 October 2019

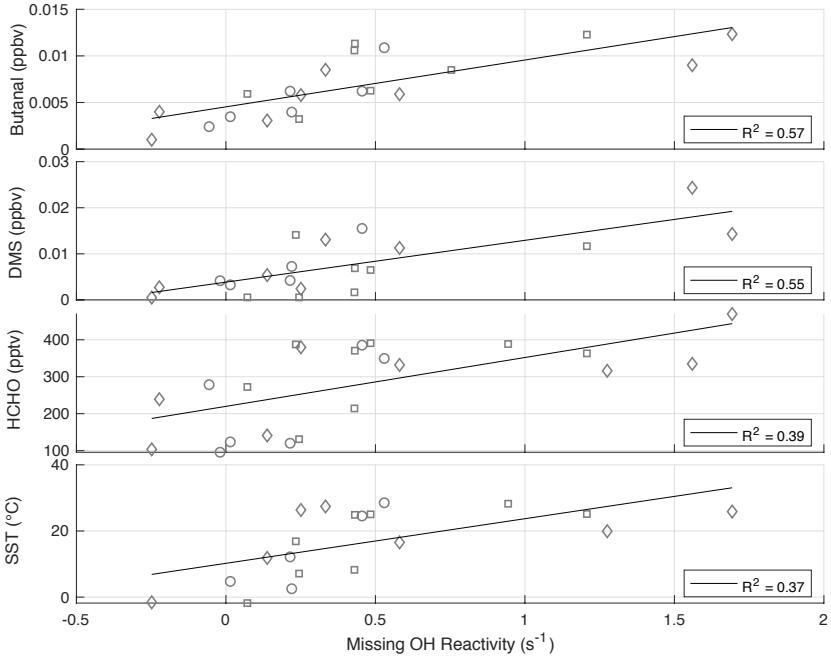

640 **Figure 8. The best correlations with missing OH reactivity at the per-flight time resolution across all latitudes and hemispheres. The symbols are values for ATom1 (circles), ATom2 (squares), ATom3 (diamonds).**

https://doi.org/10.5194/acp-2019-866
Preprint. Discussion started: 16 October 2019

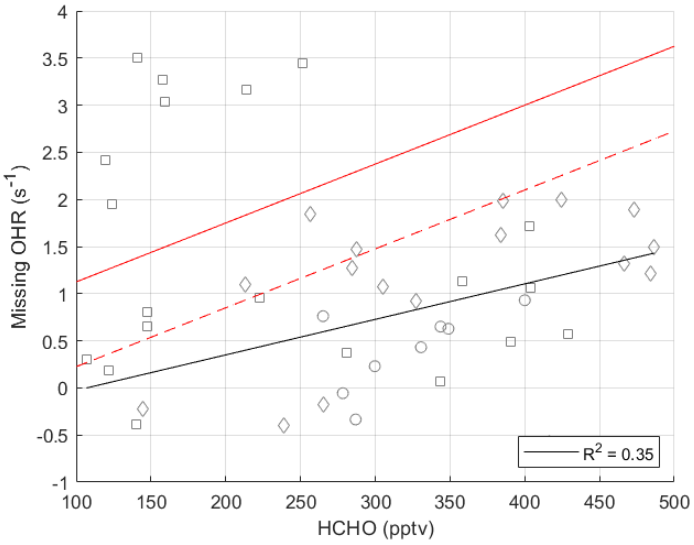

Figure 9. Missing OH reactivity against HCHO for per-dip values in the Northern Pacific hemisphere. ATom linear fit (black line) is shown with values for ATom1 (circles), ATom2 (squares), ATom3 (diamonds). The ATom linear fit is compared to the linear fit for missing OH reactivity values of Mao et. al (2009) (red line) and pressure-corrected values (red dashed line).

https://doi.org/10.5194/acp-2019-866
Preprint. Discussion started: 16 October 2019

Atmospheric Chemistry and Physics Discussions

Table 1: ATom campaign deployment seasons and start and end dates. Full details on stops can be found online (ATom, 2016).

Phase	ATom1	ATom2	ATom3	ATom4
Season	Summer	Winter	Fall	Spring
Start Date	28 July 2016	26 Jan 2017	28 Sept 2017	24 Apr 2018
End Date	22 August 2016	22 Feb 2017	26 Oct 2017	21 May 2018

https://doi.org/10.5194/acp-2019-866
Preprint. Discussion started: 16 October 2019

Atmospheric Chemistry and Physics Discussions

Table 2. Simultaneous measurements used to constrain the box model and calculate OH reactivity.

Measurement	Instrument	Uncertainty (2σ confidence)	Reference
T p	MMS	±0.5 C ± 0.3 hPa	Chan et al., 1998
H_2O	DLH	± 15%	Diskin et al., 2003
photolysis frequencies (30 measurements)	CAFS	± (12-25)%, species dependent	Shetter and Mueller, 1999
NO	NOyO3	6.6 pptv	Ryerson et al., 2000
O_3	NOyO3# UCATS	1.4 ppbv ± 1% + 1.5 ppbv	Ryerson et al., 2000
CO	QCLS# NOAA Picarro UCATS	3.5 ppbv 3.6 ppbv 8.4 ppbv	Santorini et al., 2014 H. Chen et al., 2013
H_2O_2, CH_3OOH, CH_3CO_3H, HNO_3 SO2	CIT CIMS	± 30% + 50 pptv ± 30% + 100 pptv	Crounse et al., 2006
HCOOH, BrO	NOAA CIMS	± 15% + 50 pptv	Neuman et al., 2016
CH_4	NOAA Picarro# UCATS PANTHER	0.7 ppbv 23.6 ppbv 34.6 ppbv	H. Chen et al., 2013
HCHO	NASA ISAF	± 10% ± 10 pptv	Cazorla et al., 2015
methyl nitrate, ethyl nitrate, isoprene, acetylene, ethylene, ethane, propane, i-butane, n-butane, i-pentane, n-pentane, n-hexane, n-heptane, benzene, toluene, methyl chloride, methylene chloride, chloroform, methyl bromide, methyl chloroform, perchloroethene, 1,2-dichloroethane, DMS	UCI WAS	± 10%	Colman et al., 2001
methanol, formaldehyde, acetaldehyde, ethyl benzene, toluene, methacrolein, methyl ethyl ketone, methyl tert-butyl ether, ethanol, acetone, 2-methylpentane, 3-methylpentane, 2,2,4-trimethylpentane, isobutene+1-butene, m-xylene+p-xylene, o-xylene, tricyclene, limonene+D3-carene, propanal, butanal, acrolein	TOGA	± 15-50% (acetaldehyde: ± 20%)	Apel et al., 2015

Primary measurement. Other measurements fill gaps in primary measurement.

https://doi.org/10.5194/acp-2019-866
Preprint. Discussion started: 16 October 2019

Atmospheric Chemistry and Physics Discussions

655

Table 3: Simple X photochemistry added to the photochemical mechanism to test for effects of X on modeled OH and HO_2

Reaction	Reaction rate coefficient ($cm^3\ s^{-1}$)
case 1: $X + OH \rightarrow XO_2$	$1x10^{-10}$
case 2: $X + OH \rightarrow XO_2 + OH$	
$X + O_3 \rightarrow XO_2$	$1x10^{-16}$
$XO_2 + NO \rightarrow HO_2 + NO_2 + prod$	$3x10^{-12}exp\ (300/T)$
$XO_2 + HO_2 \rightarrow XOOH$	$8.6x10^{-13}exp\ (700/T)$
$XOOH + h\upsilon \rightarrow XO + OH$	$J_{CH3OOH}\ (s^{-1})$
$XOOH + OH \rightarrow XO_2$	$2.9x10^{-12}exp\ (-160/T)$